

Spatiotemporal mapping of groundwater quality for irrigation using geostatistical analysis combined with a linear regression method

Najme Yazdanpanah¹

Received: 12 December 2015 / Accepted: 23 December 2015 / Published online: 22 January 2016
© Springer International Publishing Switzerland 2016

Abstract Spatiotemporal assessment of groundwater quality for irrigation is essential for agricultural management. This study was conducted to quantify the spatiotemporal changes of Kerman groundwater irrigation quality during 1999–2010 using geostatistical analysis combined with a new method established based on regression coefficient (RC). Result showed that among the main soluble ions, Na^+ and Cl^- had the highest concentrations. Except Ca^{+2} , the average concentration of all other soluble ions and also EC were higher than the maximum permissible levels for drinking, however, Na^+ , SO_4^{-2} and EC showed no limitations for agricultural irrigation. Based on the proposed RC, soluble Na^+ , Ca^{+2} , Cl^- , total cations, total anions and EC have gradually increased over the years. Soluble Cl^- with $0.18 \text{ meq l}^{-1} \text{ y}^{-1}$ showed averagely the highest value of RC. Also, EC exhibited an increasing trend with an average value of $16.8 \mu\text{S cm}^{-1} \text{ y}^{-1}$. In contrast, Mg^{+2} , SO_4^{-2} and SAR exhibited negative values of RC, while the value for HCO_3^- was zero. Based on nugget-to-sill ratios, the groundwater variables had moderate to strong spatial structure. Finally, the spatiotemporal changes of groundwater salinity (EC) and sodicity (SAR) have been mainly controlled by Na^+ and Cl^- .

Keywords Agriculture water · Irrigation water quality · Geostatistics · Kerman · Salinity

Introduction

Groundwater is the main source of water supply for agriculture, especially in arid and semi-arid regions (Neshat et al. 2014). Therefore, assessment of groundwater quality is considerably essential in agricultural land to facilitate groundwater planning and management (Holtz 2009; Hassanzadeh et al. 2011). The excessive exploitation of groundwater for irrigation (Yang et al. 2008), inefficient irrigation methods (Arslan 2012), irrigation with low-quality saline water (Yazdanpanah and Mahmoodabadi 2013) and uncontrolled utilization of fertilizers (Neshat et al. 2014) in agricultural lands in addition to groundwater contamination by domestic and industrial waste water (Hassanzadeh et al. 2011), have led to groundwater salinity and pollution problems. Furthermore, because of the health and economic impacts associated with groundwater contamination, the assessment of groundwater quality must be taken into consideration for sustainable groundwater protection (Hassanzadeh et al. 2011). In fact, groundwater has become the only water source in arid and semi-arid regions because of the limited availability of surface water (Yazdanpanah et al. 2011; Asadi et al. 2012; Neshat et al. 2014). Therefore, the prevention of groundwater salinity and contamination is essential for effective groundwater resource management (Guo et al. 2007).

Since, the cost of the installation and maintenance of a groundwater monitoring network is extremely high (Yang et al. 2008), geostatistical analysis provides very useful techniques for handling spatially distributed data (Nourzadeh et al. 2012; Moosavi and Sepaskhah 2012;

Electronic supplementary material The online version of this article (doi:10.1007/s40808-015-0071-9) contains supplementary material, which is available to authorized users.

✉ Najme Yazdanpanah
najmeyazdanpanah@yahoo.com

¹ Department of Water Engineering, Kerman Branch, Islamic Azad University, P.O. Box: 7635131167, Kerman, Iran

Mousavifard et al. 2013). This approach has been applied for the interpolation and mapping of water level (Kumar 2007; Theodossiou and Latinopoulos 2007; Yang et al. 2008; Sun et al. 2009; Dash et al. 2010; Yimit et al. 2011) as well as water quality and pollution (Gaus et al. 2003; Ghosh et al. 2004; Demir et al. 2009; Delgado et al. 2010; Nas and Berktaş 2010; Baalousha 2010; Mendes and Ribeiro 2010; Arslan 2012). Also, geostatistical analysis plays an important role in the management and sustainability of regional water resources (Demir et al. 2009; Baalousha 2010; Dash et al. 2010). In this context, geostatistical methods can be combined in a geographical information system (GIS) framework to map the spatial distribution of groundwater characteristics (Theodossiou and Latinopoulos 2007; Neshat et al. 2014). In addition, the investigation of both spatial and temporal changes of groundwater variables has been reported in the literature (Sun et al. 2009; Arslan 2012).

Kriging is a geostatistical interpolation technique, which includes a number of methods such as simple Kriging, ordinary Kriging, co-Kriging, stratified Kriging and non-linear Kriging (Nazarizadeh et al. 2006; Yang et al. 2008; Zehtabian et al. 2010; Yimit et al. 2011). Gaus et al. (2003) used disjunctive Kriging to interpolate the probability and concentration of arsenic concentrations in groundwater of Bangladesh. Theodossiou and Latinopoulos (2007) evaluated groundwater observation networks using the Kriging methodology to interpolate groundwater levels in the Anthemountas basin of northern Greece. Kuusi et al. (2009) used Kriging methods to assess the spatial variability of groundwater nitrate and salinity in the Amman-Zarqa Basin. Zehtabian et al. (2010) provided spatial distribution maps for some groundwater cations and anions in Garmsar watershed of Iran. Yimit et al. (2011) applied ordinary Kriging to map groundwater levels and salinity in Xinjiang, northwest China. Groundwater quality zonation was performed by Maghami et al. (2011) in Abadeh township of Iran using different geostatistical methods and finally Kriging was found as the best method for mapping the quality of drinking water in the study area.

Kerman plain in southeast part of Iran has been faced with severe groundwater problems. In this area, groundwater is the main resource of agricultural and municipal water supply. However, water table has continuously lowered in upper-lands due to excessive pumping of groundwater during the last two to three decades, so that more than 16 m drawdown in the aquifer happened during recent 20 years (Rezaei 2013). Pistachio (*Pistacia vera*) is the main cultivation in the region (Yazdanpanah et al. 2013) and fertilizers have been extensively used. From another point of view, the entrance of domestic and municipal wastewaters into the groundwater of lower-lands where Kerman city has been established has led to water raising and aquifer

contamination (Hasanpour et al. 2011). These concerns underlie the importance of investigating groundwater vulnerability in the Kerman plain. Therefore, the objectives of this study were (1) to determine the most appropriate Kriging model for mapping the groundwater quality for irrigation in Kerman plain, and (2) to investigate the spatial and temporal changes in some chemical groundwater variables from 1999 to 2010. For this purpose, a new approach was proposed to model the spatiotemporal variability of the groundwater irrigation quality and finally the rate of changes over the years was quantified.

Materials and methods

Study area description

This study was performed in Kerman plain located between $56^{\circ} 30' - 57^{\circ} 30' \text{ E}$ and $29^{\circ} 50' - 30^{\circ} 30' \text{ N}$ with an area of 5478 km^2 , in an arid to semi-arid region in southeast Iran (Fig. 1). The elevation varies from 1700 to 1950 m a.s.l., sloping from south and south east toward the central and north western parts of the plain with a similar direction for the groundwater level. Figure 2 shows groundwater levels of the plain for the last year i.e. 2010 and the position of Kerman city and other urban areas. A long-term mean precipitation of the area is 140 mm per annum, which mainly occurs in winter. During the recent 25 years, the maximum and minimum amounts of rainfall have been recorded for years 1992 ($307.2 \text{ mm year}^{-1}$) and 1998 ($56.3 \text{ mm year}^{-1}$). The average annual temperature for this region is 16.5°C and varies from 1.9 to 28.9°C . At the north central side of the plain, Kerman city is located on a fine grain bed rock with low permeability leading to water accumulation beneath the city. This city with an area of $15,000 \text{ ha}$ is one of the largest cities in south east of Iran, with a population of more than 530,000 (The Planning and Management Organization of Kerman Province 2011). In Kerman a majority of houses have absorption wells, which are the main sewage disposal method (Hassanzadeh et al. 2011), resulting in the groundwater pollution by domestic waste water.

Kerman plain is mostly composed of Cretaceous limestone covered by Quaternary deposits i.e. alluvial, evaporative and Aeolian sediments (Hassanzadeh et al. 2011). In general, there are two major geological facieses in the region (Hasanpour et al. 2011). First, limestone and dolomite in the eastern part of Kerman plain, which are contributing to the aquifer's recharge and second, marl facieses in the western part, which are consisting of evaporative sediments and leading to the groundwater salinity. According to the excavation of discovery wells and seismic studies (Aminizadeh et al. 2012), the thickness of the

Fig. 1 The location of Kerman plain on Iran map

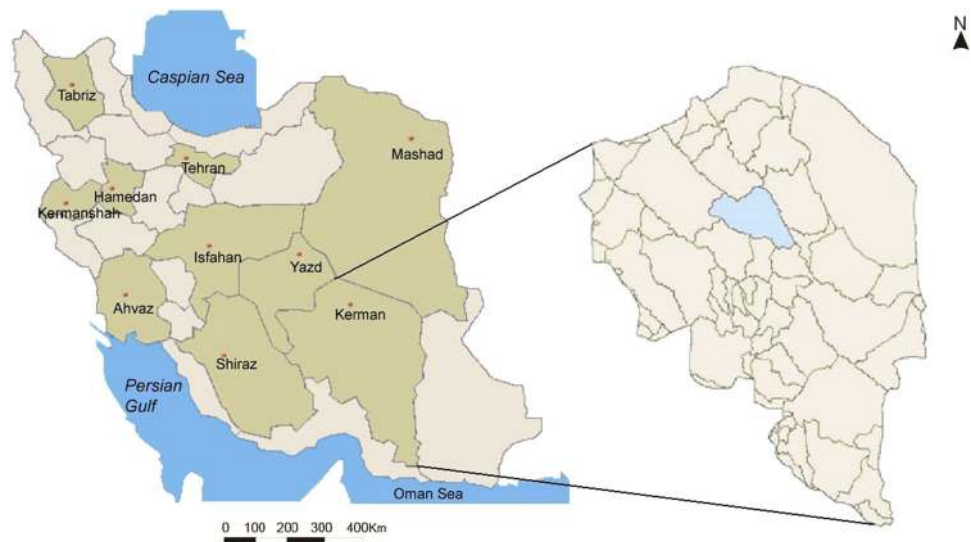
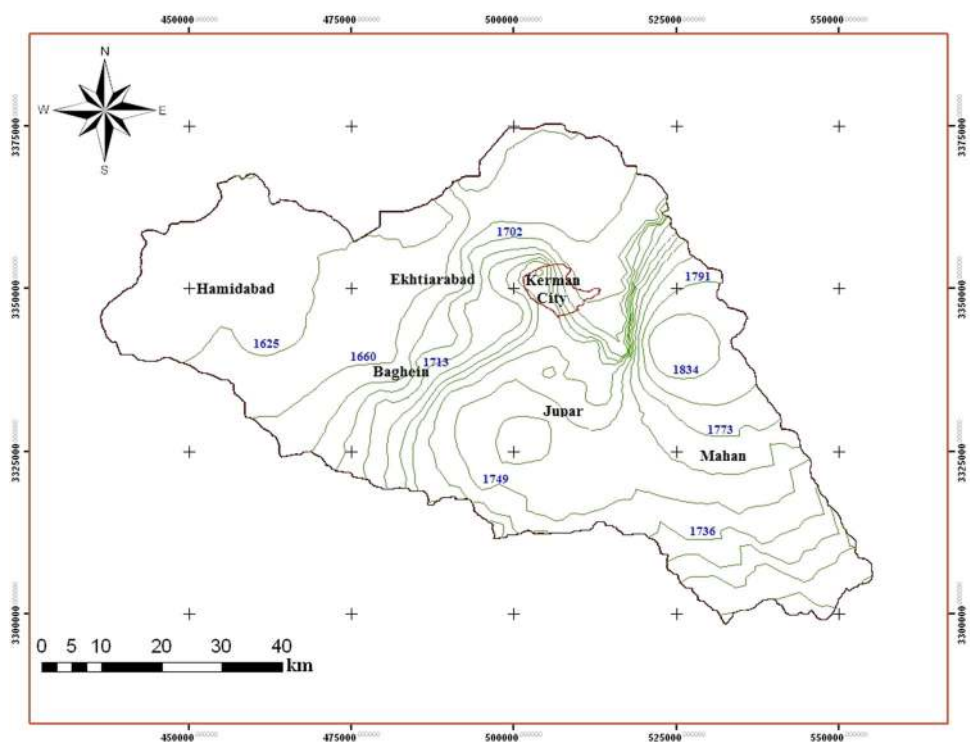


Fig. 2 Groundwater levels of Kerman aquifer for year 2010 and the position of Kerman city and other urban areas



sediments is varied from 30 to 350 m. The depth of the bed rock in south east and central parts of the plain is about 250 m, whereas, in other regions it varied between 130 and 150 m. Also, there is a deep basin underground in the west part of Kerman city.

Database preparation

In this study, groundwater quality data of 56 agricultural wells were collected from the Water Organization of

Kerman. For each well, the concentrations of main soluble ions including sodium (Na^+), calcium (Ca^{+2}), magnesium (Mg^{+2}), total cations, chloride (Cl^-), bicarbonate (HCO_3^-), sulfate (SO_4^{-2}), total anions, and the values of electrical conductivity (EC) as well as sodium adsorption ratio (SAR) were obtained for years 1999–2010. Summary statistics for each groundwater variable were generated and then, a normality (Kolmogorov–Smirnov) test was conducted to assess the normal distribution of each one. Accordingly, the database was prepared using the obtained

data for each groundwater variable. The value of each groundwater variable was compared with the maximum permissible levels for drinking and agriculture based on Environmental Protection Organization of Iran (2001) and the United States Environmental Protection Agency (2012).

To quantify the temporal changes of the selected groundwater variables over the studied period of years, a new approach was proposed. This method is established based on the regression coefficient concept. A regression equation can be used to predict the values of one variable knowing those of one or more others. In general, when a regression line is considered as linear (i.e. $y = ax + b$), the regression coefficient is a constant (a), which represents the rate of change of each groundwater variable (y) as a function of time (x); it is the slope of the regression line (Webster 1997). Therefore, the values of each groundwater variable against the corresponding years (from 1999 to 2010) were plotted and the best linear trend line was fitted. Then, the regression coefficient (a) was determined as a constant value for each groundwater variable, hereafter called “RC”. Negative value of RC for each groundwater variable implies that the variable over time (years) has been reduced and vice versa.

Geostatistical analysis

Geostatistical analysis of data was performed in two stages including (1) the structural analysis, which aims at describing and modeling the spatial structure of the RC parameter for the groundwater variables, using a structural tool i.e. variogram; (2) the use of this structure for a given evaluation problem (e.g. to make up the maps of each groundwater RC parameter). In this study, some geostatistical algorithms including ordinary, simple, universal, indicator, probability, and disjunctive Kriging were tested (ESRI 2008). Through the analysis of the semi-variogram, the best model (e.g., spherical, exponential, or Gaussian) and the relevant parameters (nugget, sill, and range) were determined. According to variography analysis, spatiotemporal groundwater quality maps were derived for each variable.

According to the theoretical basis (ESRI 2008), the main tool in geostatistics is variogram, which expresses the spatial dependence between neighboring observations. The variogram, γ_h , can be defined as one-half the variance of the difference between attribute values at all points separated by h as (Li and Heap 2008):

$$\gamma_h = \frac{1}{2n} \sum_{i=1}^n [Z(x_i) - Z(x_i + h)]^2 \quad (1)$$

where γ_h is the semi-variance value for all pairs at a lag distance h ; $Z(x_i)$ is the regression coefficient (RC) of the

selected groundwater variable at point i ; $Z(x_i + h)$ is the RC value of the groundwater variable for other points separated from x_i by a discrete distance h ; x_i is the geo-referenced position where the $Z(x_i)$ value is measured; n represents the number of pairs of observations separated by the distance h .

Model validation

Prediction performances of the interpolation models were assessed by cross-validation. Basically, the input data were split into two subsets. The first subset of the available data was used to develop a model for prediction. The predicted values were then compared with the known values at the remaining locations using the validation tool. The effectiveness of subsequent interpolation efforts was evaluated based on relative root mean square error (RMSE) and also using mean absolute error (MAE) and mean bias error (MBE) parameters (Park and Vlek 2002):

$$RMSE = \sqrt{\frac{\sum_{i=1}^n [Z \times (x_i) - Z(x_i)]^2}{n}} \quad (2)$$

$$MAE = \frac{\sum_{i=1}^n |Z \times (x_i) - Z(x_i)|}{n} \quad (3)$$

$$MBE = \frac{\sum_{i=1}^n [Z \times (x_i) - Z(x_i)]}{n} \quad (4)$$

where $Z \times (x_i)$ is the predicted value at point x_i , $Z(x_i)$ is the observed value at point x_i , and n is the number of observations. Smaller values of the RMSE, MAE and MBE indicate that the estimated values are closer to the observed values. By this procedure, the best predictive model was selected to create spatiotemporal distribution maps for each groundwater variable.

Results and discussion

Descriptive statistics

Table 1 shows the amounts of groundwater variables of Kerman plain in comparison with the maximum permissible levels for drinking and agriculture irrigation. Among the studied cations and anions, soluble Na^+ with an average of 15.94 meq l^{-1} and Cl^- with an average of 14.53 meq l^{-1} showed the highest concentrations in the groundwater. As is clear, the average concentrations of Na^+ and SO_4^{2-} in addition to the amount of EC were higher than the maximum permissible levels for drinking,

Table 1 Summary statistics of groundwater quality variables for Kerman plain aquifer based on 56 observation wells in comparison with the maximum permissible levels for drinking and agriculture

Variable	Average	Minimum	Maximum	Standard deviation	Max permissible level for drinking	Max permissible level for agriculture
Na ⁺ (meq l ⁻¹)	15.94	0.84	113.29	19.87	7.61	39.13
Ca ⁺² (meq l ⁻¹)	4.72	1.18	17.46	3.27	5.00	10.00
Mg ⁺² (meq l ⁻¹)	6.48	1.24	28.83	5.39	6.17	2.47
Cations (meq l ⁻¹)	27.13	4.06	159.57	27.20	–	–
Cl ⁻ (meq l ⁻¹)	14.53	0.46	112.43	18.85	7.04	14.08
HCO ₃ ⁻ (meq l ⁻¹)	4.19	1.76	11.83	1.90	–	9.84
SO ₄ ⁻² (meq l ⁻¹)	8.38	0.81	41.34	8.49	2.60	9.90
Anions (meq l ⁻¹)	27.10	4.06	159.00	27.10	–	–
EC (μS cm ⁻¹)	2468.0	382.3	13792.9	2356.91	2000	2700
SAR (meq l ⁻¹) ^{0.5}	5.99	0.65	23.60	4.85	–	–

The maximum permissible levels are presented based on Environmental Protection Organization of Iran (2001) and the United States Environmental Protection Agency (2012). For equivalence and comparison, the unit of permissible values was converted from mg l⁻¹ to meq l⁻¹

Table 2 Area distribution of soluble cations within different classes in groundwater of Kerman plain

Na ⁺ (meq l ⁻¹)			Ca ⁺² (meq l ⁻¹)			Mg ⁺² (meq l ⁻¹)			Total Cations (meq l ⁻¹)		
Class	Area (km ²)	Area (%)	Class	Area (km ²)	Area (%)	Class	Area (km ²)	Area (%)	Class	Area (km ²)	Area (%)
0.8–3.3	85.54	1.56	1.2–1.7	0	0.00	1.2–2.1	19.36	0.35	4.1–8.2	48.32	0.88
3.3–4.6	296.96	5.42	1.7–2.1	40.00	0.73	2.1–2.6	44.37	0.81	8.2–10.7	133.57	2.44
4.6–5.4	250.49	4.57	2.1–2.6	121.09	2.21	2.6–2.9	44.50	0.81	10.7–12.2	108.59	1.98
5.4–6.7	388.09	7.08	2.6–3.3	547.16	9.99	2.9–3.4	91.12	1.66	12.2–14.6	266.14	4.86
6.7–9.2	634.33	11.58	3.3–4.3	999.83	18.25	3.4–4.3	222.77	4.07	14.6–18.9	521.07	9.51
9.2–13.7	950.34	17.35	4.3–5.6	2466.99	45.03	4.3–5.7	780.09	14.24	18.9–26.1	934.93	17.07
13.7–21.8	1444.76	26.37	5.6–7.4	1030.94	18.82	5.7–8.1	3796.52	69.30	26.1–38.6	2862.29	52.25
21.8–36.7	1126.90	20.57	7.4–9.8	216.18	3.95	8.1–11.9	383.18	6.99	38.6–60.1	489.04	8.93
36.7–63.8	300.65	5.49	9.8–13.1	55.87	1.02	11.9–18.3	96.15	1.76	60.1–96.6	114.11	2.08
>63.8	0	0.00	>13.1	0	0.00	>18.3	0	0.00	>96.6	0	0.00

however they showed no limitation for agricultural water usage. On average, Ca⁺² had lower concentration than the maximum permissible values for drinking and agriculture, whereas, the average concentrations of Mg⁺² and Cl⁻ were greater than the maximum permissible values. This means that among the studied variables, only the concentration of Ca⁺² was less than permissible levels, whereas the other ones showed critical values particularly for drinking water usage. Dash et al. (2010) in studying groundwater quality parameters in Delhi found that Cl⁻ levels in 62 % and EC values in 69 % of the area exceeded the permissible thresholds. The result of Hassanzadeh et al. (2011) indicated that the concentration of some major ions including Na⁺, Ca⁺², Mg⁺², K⁺, Cl⁻, SO₄⁻² and EC in groundwater of an urban area exceeded the maximum permissible level for drinking water, which was ascribed to enrichment beneath the city. The groundwater EC value is ranging

from 382.3 to 13792.9 μS cm⁻¹. The large variation in EC is mainly attributed to geochemical processes prevailing in this region (Pazand and Javanshir 2014).

Tables 2, 3 and 4 show the distribution of soluble cations, anions as well as EC and SAR within different classes in groundwater of Kerman aquifer. Overall, 75.87 % of the area had Na⁺ values in the range of 6.7–36.7 meq l⁻¹, 82.1 % of the aquifer showed Ca⁺² concentrations ranging from 3.3 to 7.4 meq l⁻¹ and 83.54 % of the area had Mg⁺² values in the range of 4.3–8.1 meq l⁻¹. Also, the dominate class of Cl⁻ was 6.3–36.2 meq l⁻¹ (85.82 % of the area), 68.04 % of the region had HCO₃⁻ values ranging from 3.6 to 5.2 meq l⁻¹, and 67.83 % of the study area showed SO₄⁻² values varying from 6.9 to 13.2 meq l⁻¹. Furthermore, 81.90 % of the study area had EC values higher than 1769 μS cm⁻¹, whereas the most dominant SAR values (68.30 %) were

Table 3 Area distribution of soluble anions within different classes in groundwater of Kerman plain

Cl ⁻ (meq l ⁻¹)			HCO ₃ ⁻ (meq l ⁻¹)			SO ₄ ⁻² (meq l ⁻¹)			Total Anions (meq l ⁻¹)		
Class	Area (km ²)	Area (%)	Class	Area (km ²)	Area (%)	Class	Area (km ²)	Area (%)	Class	Area (km ²)	Area (%)
0.4–2.9	39.81	0.73	1.7–2.5	153.76	2.81	0.8–2.4	0	0.00	4.1–7.9	29.79	0.54
2.9–4.2	156.86	2.86	2.5–3.1	411.72	7.52	2.4–3.5	232.44	4.24	7.9–10.2	93.19	1.70
4.2–4.9	110.35	2.01	3.1–3.4	298.02	5.44	3.5–4.2	234.93	4.29	10.2–11.5	60.22	1.10
4.9–6.3	325.41	5.94	3.4–3.6	239.53	4.37	4.2–5.3	324.86	5.93	11.5–13.7	252.55	4.61
6.3–8.7	728.04	13.29	3.6–3.9	575.06	10.50	5.3–6.9	533.64	9.74	13.7–17.6	479.4	8.75
8.7–13.2	1317.09	24.04	3.9–4.4	1797.18	32.81	6.9–9.4	2612.14	47.68	17.6–24.5	764.28	13.95
13.2–21.4	2001.61	36.54	4.4–5.2	1354.74	24.73	9.4–13.2	1103.57	20.15	24.5–36.5	3096.05	56.52
21.4–36.2	654.88	11.95	5.2–6.5	379.99	6.94	13.2–19.1	381.51	6.96	36.5–57.6	576.31	10.52
36.2–63.2	144.01	2.63	6.5–8.5	268.06	4.89	19.1–27.9	54.97	1.00	57.6–94.5	126.27	2.31
>63.2	0	0.00	>8.5	0	0.00	>27.9	0	0.00	>94.5	0	0.00

Table 4 Area distribution of EC and SAR within different classes in groundwater of Kerman plain

EC (μS/cm)			SAR (meq l ⁻¹) ^{0.5}		
Class	Area (km ²)	Area (%)	Class	Area (km ²)	Area (%)
382–774	46.06	0.84	0.6–1.9	8.30	0.15
774–1007	117.12	2.14	1.9–2.5	71.68	1.31
1007–1145	109.61	2.00	2.5–2.8	66.25	1.21
1145–1378	214.23	3.91	2.8–3.1	95.67	1.75
1378–1769	504.85	9.22	3.1–3.3	72.25	1.32
1769–2428	1280.00	23.37	3.3–4.1	346.18	6.32
2428–3535	2689.21	49.09	4.1–5.2	528.47	9.65
3535–5397	397.28	7.25	5.2–7.8	3741.44	68.30
5397–8528	119.70	2.19	7.8–13.1	443.94	8.10
>8528	0	0.00	13.1–23.6	103.88	1.90

observed in class 5.2–7.8 (meq l⁻¹)^{0.5}. In fact, a considerable percent of the aquifer exhibited salinity limitations with EC values more than 2250 μS cm⁻¹ and little danger of developing harmful levels of sodium. Therefore, this part of groundwater cannot be used for irrigation of soils of restricted drainage. Even with adequate drainage, special management for salinity control including provision for high degree of adverse effects may be required and agricultural crops of very salt tolerance can be cultivated. Kotuby et al. (1997) concluded that EC levels over 2250 μS cm⁻¹ can lead to yield reductions of about 50 % for rice, tomato, peppers, spinach and corn.

As illustrated above, a new approach was offered for modeling the spatiotemporal changes of groundwater properties with time (year) based on the regression coefficient (RC). The value of RC obtained for each groundwater property represents the slope changes with time. Positive values indicate an increase in the amount of each groundwater variable over years and vice versa. Table 5 shows the average, minimum and maximum values of RC

Table 5 Summary statistics of the regression coefficient (RC) for the groundwater properties in the study area

Variable	Average	Minimum	Maximum
Na ⁺ (meq l ⁻¹ year ⁻¹)	0.03	−1.59	1.61
Ca ⁺² (meq l ⁻¹ year ⁻¹)	0.15	−0.34	1.49
Mg ⁺² (meq l ⁻¹ year ⁻¹)	−0.11	−1.47	0.73
Cations (meq l ⁻¹ year ⁻¹)	0.15	−2.04	3.02
Cl ⁻ (meq l ⁻¹ year ⁻¹)	0.18	−1.07	3.00
HCO ₃ ⁻ (meq l ⁻¹ year ⁻¹)	0.00	−0.24	0.58
SO ₄ ⁻² (meq l ⁻¹ year ⁻¹)	−0.10	−3.05	1.51
Anions (meq l ⁻¹ year ⁻¹)	0.09	−1.98	3.07
EC (μS cm ⁻¹ year ⁻¹)	16.8	−108.1	299.1
SAR [(meq l ⁻¹) ^{0.5} year ⁻¹]	−0.01	−0.73	0.58

Negative value of RC for each groundwater property implies that the property over time (year) is gradually becoming smaller and vice versa

for each groundwater variable in the study Kerman plain. The result showed that Na⁺, Ca⁺², Cl⁻, total cations, total anions and EC had on average positive values of RC. In

fact, these groundwater variables have gradually increased during 1999–2010. Among the main soluble ions, Cl^- showed the highest increase with an average RC value of $0.18 \text{ meq l}^{-1} \text{ y}^{-1}$. Also, the EC of groundwater showed an increasing trend with an average of $16.8 \mu\text{S cm}^{-1} \text{ y}^{-1}$. The value of RC for HCO_3^- was zero, indicating no changes through the studied years. In contrast, Mg^{+2} and SO_4^{-2} with respectively -0.11 and $-0.10 \text{ meq l}^{-1} \text{ y}^{-1}$ and SAR with $-0.01 (\text{meq l}^{-1})^{0.5} \text{ y}^{-1}$ exhibited negative values of RC. However, these values of RC represent the average time changes for the whole aquifer, while ranged between negative and positive values.

Varogram analysis

Classical statistics are not necessarily suitable for analysis of variation patterns of every variable, because groundwater properties often exhibit spatial dependence. Also, each groundwater variable can be modeled as a function of time (year). Therefore, to determine the spatiotemporal behavior of the groundwater properties, the spatial dependency of regression coefficient (RC) for each property was modeled using analysis of semi-variance. By this way, both spatial and temporal variability of the groundwater variables were quantified. Table 6 presents the semi-variogram model parameters of the RC for different water quality variables as well as cross validation result in the study area obtaining for years 1999–2010. The result indicated that the best method for interpolation of Na^+ , Mg^{+2} , Cl^- , HCO_3^- and SAR was disjunctive Kriging, whereas for Ca^{+2} , total cations, total anions and EC simple Kriging found to be the best method. In addition, the performance of ordinary Kriging resulted in a better interpolation for SO_4^{-2} .

The variography analysis indicated that Exponential model for Na^+ , Cl^- , SO_4^{-2} , total cations and SAR, the Gaussian model for Ca^{+2} and Mg^{+2} , and the Spherical

model for HCO_3^- , total anions and EC were the most satisfactory predictors. Nazarizadeh et al. (2006) found that the variograms of EC, Cl^- and SO_4^{-2} best fit with the spherical model. In another research, Maghami et al. (2011) performed groundwater quality zonation using 27 observed wells in Abadeh Township, with an unconfined aquifer. Their result showed that the Kriging method with an exponential semi-variogram was the best method for interpolating the quality of drinking water.

Our result also showed that the nugget ranged from 0 to 0.47 for the main soluble ions, while it was found to be 1513 and 0.67 for EC and SAR, respectively. The nugget is mainly caused by small scale variations, or sometimes just by measurement errors. With the nugget effect, the Kriging weights become similar and the variance of estimation error increases. If there is no nugget effect, the average standard deviation generally decreases with the increase of the number of observation wells (Yang et al. 2008).

Sill is a constant value for bounded variograms or an asymptotic value for unbounded variograms (Webster and Oliver 2001). With the same number of observation wells, the average standard deviation is large for large sill value. Therefore, for a given maximum tolerable average standard deviation, more observation wells are required for the case with large sill values (Yang et al. 2008). Our result indicated that the minimum and maximum values of sill obtained for Ca^{+2} and Na^+ with the amounts of 0.12 and 1.34, respectively. Sill values for EC and SAR were 4096 and 1.17, respectively.

The nugget-to-sill ratio, which is also known as the relative nugget variance, can determine the grade of the spatial dependence of any variable. Spatial dependence of groundwater variables was classified according to nugget-to-sill ratio (%), with a ratio of $<25\%$ indicating a strong spatial dependence, a ratio of $25\text{--}75\%$ indicating moderate spatial dependence and a ratio of $>75\%$ indicating a weak spatial dependence (Kravchenko 2003; Rossi et al. 2009;

Table 6 Semi-variogram model parameters of the regression coefficient (RC) for different water quality properties in the study area

Variable	Geostatistical algorithm	Model	Nugget (C0)	Partial sill (C)	Sill (C0 + C)	Range (m)	Spatial dependency	RMSE	MAE	MBE
Na^+	Disjunctive Kriging	Exponential	0.21	1.13	1.34	7970	Strong	0.51	0.34	0.01
Ca^{+2}	Simple Kriging	Gaussian	0.05	0.07	0.12	15,038	Moderate	0.31	0.21	-0.01
Mg^{+2}	Disjunctive Kriging	Gaussian	0.47	0.54	1.01	9096	Moderate	0.33	0.23	0.01
Cations	Simple Kriging	Exponential	0.04	0.65	0.69	12,009	Strong	0.69	0.44	0.02
Cl^-	Disjunctive Kriging	Exponential	0.08	0.46	0.54	31,273	Strong	0.50	0.3	0.007
HCO_3^-	Disjunctive Kriging	Spherical	0.43	0.79	1.22	23,116	Moderate	0.14	0.09	0.007
SO_4^{-2}	Ordinary Kriging	Exponential	0	0.65	0.65	12,496	Strong	0.71	0.43	0.01
Anions	Simple Kriging	Spherical	0.07	0.69	0.76	10,733	Strong	0.72	0.48	0.02
EC	Simple Kriging	Spherical	1513	2583	4096	14,225	Moderate	56.23	37.72	0.45
SAR	Disjunctive Kriging	Exponential	0.67	0.50	1.17	65,703	Moderate	0.22	0.15	0.0008

Wang et al. 2009; Arslan 2012). Findings for nugget-to-sill ratios in the present study indicated the groundwater variables to have moderate to strong spatial structure. Overall, small nugget-to-sill ratios and large spatial correlation ranges usually indicate that high accuracy can be achieved when mapping a variable (Isaaks and Srivastava 1989).

The effective range is the distance beyond which the variogram value remains essentially constant. The larger the range is, the stronger the spatial correlation is (Webster and Oliver 2001). According to Table 6, the minimum and maximum ranges were found for Na^+ and SAR with the values of 7970 and 65,703 m, respectively. Zehtabian et al. (2010) in modeling of Garmsar groundwater quality reported that the best fit model for total cations, total anions and SO_4^{2-} was similarly spherical with a range of 51,100 m, whereas a linear model with a range of 20,896 m found to be the best for HCO_3^- . The range obtained by Nazarizadeh et al. (2006) in Balaroud groundwater for EC, Cl^- and SO_4^{2-} was 61,700, 50,800 and 102,100 m, respectively.

The cross-validation statistics given in Table 6 show how well groundwater variables can be estimated by application of the selected Kriging interpolation models. Smaller values of RMSE, MAE and MBE indicate that the estimated values are closer to the observed values. The result showed that for the main soluble ions the values of RMSE and MAE ranged from 0.14 to 0.72 and from 0.09 to 0.48, respectively. The values of these two parameters obtained for the groundwater EC were respectively 56.23 and 37.72. Moreover, cross-validation result showed that MBE values to be close to 0, i.e. between -0.01 and 0.02 for the main soluble ions and 0.45 for EC, indicating an accuracy of predictions (Sun et al. 2009).

Spatial mapping

Once cross-validated, the parameters of the semi-variogram models were used in the construction of spatiotemporal groundwater quality maps for irrigation by the selected geostatistical methods. In other words, the prepared maps show the spatial variability of the RC parameter, which by itself represents the temporal changes of each groundwater property at every point during 1999–2010. In this regard, three groups of maps including (1) soluble cations, (2) soluble anions and (3) EC and SAR were generated (Figs. 3, 4, 5).

According to Fig. 3a, most of the study area allocated to class 0.01 – $0.05 \text{ meq l}^{-1} \text{ year}^{-1}$. Instead, spatial changes of RC parameter for Na^+ in the north central and western parts of the plains, especially beneath the city had no clear pattern. According to Table 5, the average RC for soluble Na^+ was $0.03 \text{ meq l}^{-1} \text{ year}^{-1}$, varying between -1.59 and $1.61 \text{ meq l}^{-1} \text{ year}^{-1}$. Spatiotemporal variability map of

soluble Ca^{+2} is shown in Fig. 3b. The dominant class of RC parameter was 0.12 – $0.27 \text{ meq l}^{-1} \text{ year}^{-1}$, indicating an increasing trend in the concentration of Ca^{+2} during 1999–2010 in most area of the aquifer. However, some negative values of RC parameter were observed in the central part of the plain, where the city has been developed. The value of RC for Ca^{+2} varied from -0.34 to 1.49 with an average of $0.15 \text{ meq l}^{-1} \text{ year}^{-1}$. Spatial changes of RC parameter for groundwater Mg^{+2} (Fig. 3c) indicated that most areas of the aquifer are placed in class -0.15 to $-0.08 \text{ meq l}^{-1} \text{ year}^{-1}$. Unlike Na^+ and Ca^{+2} , the soluble Mg^{+2} exhibited a decreasing trend over the years with an average RC value of -0.11 ranging from -1.47 to $0.73 \text{ meq l}^{-1} \text{ year}^{-1}$ (Table 5). Most irregularities in the spatial changes of Mg^{+2} were observed in the central and western parts of the aquifer. The prepared map of spatial changes of RC for total cations (Fig. 3d) was relatively similar to that one obtained for Ca^{+2} with an average of $0.15 \text{ meq l}^{-1} \text{ year}^{-1}$. The most abundant values of RC parameter were classified in the range of 0.05 – $0.35 \text{ meq l}^{-1} \text{ year}^{-1}$. In general, the north central and western parts of Kerman aquifer showed different patterns of spatiotemporal variability from the other areas.

The concentration of soluble Cl^- showed the highest reductions in central as well as western parts of the study area (Fig. 4a). According to Table 5, the average value of RC was $0.18 \text{ meq l}^{-1} \text{ year}^{-1}$, ranging from -1.07 to $3.0 \text{ meq l}^{-1} \text{ year}^{-1}$. In most area of the Kerman groundwater, the average value of RC obtained for HCO_3^- was equal to or less than zero, indicating that the concentration of this anion had no increasing trend from 1999 to 2010 (Fig. 4b). However, beneath the city region, positive values of RC parameter were observed. A plausible reason for increasing the concentration of HCO_3^- in this area can be due to organic substance degradation in domestic waste water (Hassanzadeh et al. 2011). In another study, geogenic (Fe-oxides, calcareous rocks with phosphorite intercalations, ophiolite fragments within deltaic deposits) and anthropogenic contamination sources (intensive agricultural and farming practices) were found to control the spatial distribution of some elements in stream sediments of Arta plain (Papadopoulou-Vrynioti et al. 2013). Our result showed that in the residential areas, the value of RC parameter for SO_4^{2-} was negative (Fig. 4c). The average value of RC was $-0.1 \text{ meq l}^{-1} \text{ year}^{-1}$, ranging from -3.05 to $1.51 \text{ meq l}^{-1} \text{ year}^{-1}$. Anyway, more irregularities in spatiotemporal patterns of SO_4^{2-} than in the other ions were observed. The result also implied that the RC parameter for total anions ranged from -1.98 to $3.07 \text{ meq l}^{-1} \text{ year}^{-1}$ with an average value of $0.09 \text{ meq l}^{-1} \text{ year}^{-1}$. Most of the area allocated to class -0.07 to 0.11 (Fig. 4d). Meanwhile, some negative and positive values of RC parameter were observed in the north central and western parts of the plain.

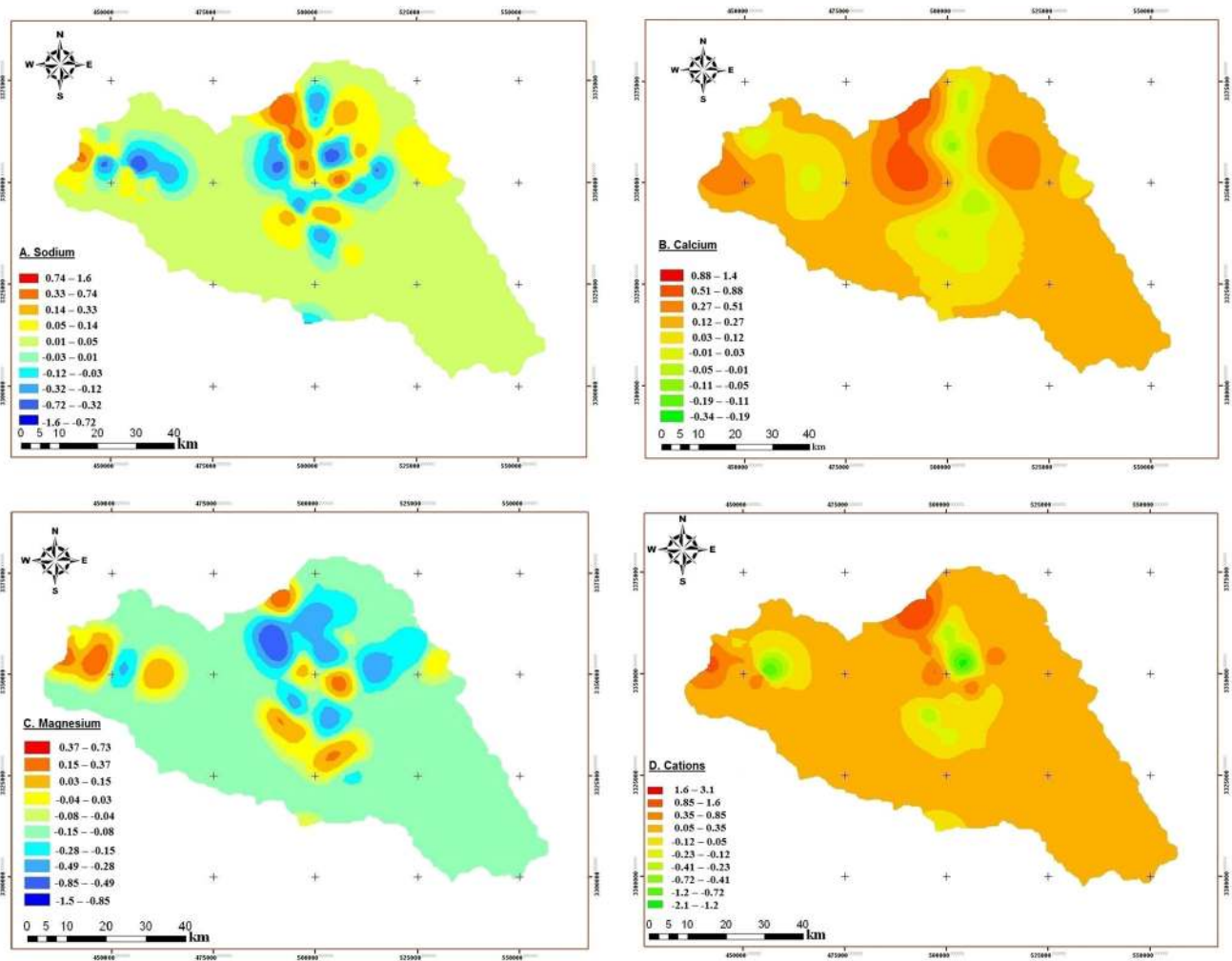


Fig. 3 Spatiotemporal mapping of RC parameter for soluble cations in Kerman aquifer including sodium (a), calcium (b), Magnesium (c) and total cations (d)

Figure 5a shows the spatiotemporal variability of EC for irrigation in the aquifer. The dominant class of RC parameter for EC was $8.6\text{--}18.9\ \mu\text{S cm}^{-1}\text{ year}^{-1}$. It is obvious that some parts in north central and western parts of the plain exhibited negative values of RC. Based on Table 5, the range of RC parameter for groundwater EC varied from -108.1 to $299.1\ \mu\text{S cm}^{-1}\text{ year}^{-1}$ with an average value of $16.8\ \mu\text{S cm}^{-1}\text{ year}^{-1}$. The spatiotemporal variability of groundwater SAR differed from the soluble ions, so that toward the western parts of the plain, the negativity of RC parameter intensified. This trend can be ascribed to the reduction of soluble Na^+ as well as increases in Ca^{+2} and Mg^{+2} in the west part (Fig. 3). The value of RC parameter for groundwater SAR ranged from -0.73 to $0.58\ (\text{meq l}^{-1})^{0.5}\text{ year}^{-1}$, with an average of $-0.01\ (\text{meq l}^{-1})^{0.5}\text{ year}^{-1}$.

Comparison of the main soluble ions indicated that during 1999–2010, the concentration of HCO_3^- has been increased beneath the Kerman city, whereas the reverse

manner was found for Ca^{+2} and SO_4^{-2} . The increase of HCO_3^- may be due to human activities and the consequent groundwater enrichment by domestic waste water. The reverse manner for Ca^{+2} and SO_4^{-2} is partly as a result of raised groundwater level and the entrance of water and waste water with relatively low amounts of these ions into the ground water (Hasanpour et al. 2011). The spatial distribution of water Cl^- concentrations and EC values for agricultural use in the Arta plain showed that sea water intrusion was responsible for its elevated salt contents in the coastal area (Papadopoulou-Vrynioti et al. 2014). Our result indicated that in the north central part of the plain where the urban areas have been developed, the most irregularity in the spatiotemporal changes of the groundwater properties was found. This can be attributed to the groundwater enrichment by domestic waste water due to human activities combined with the weathering of evaporates such as halite and gypsum.

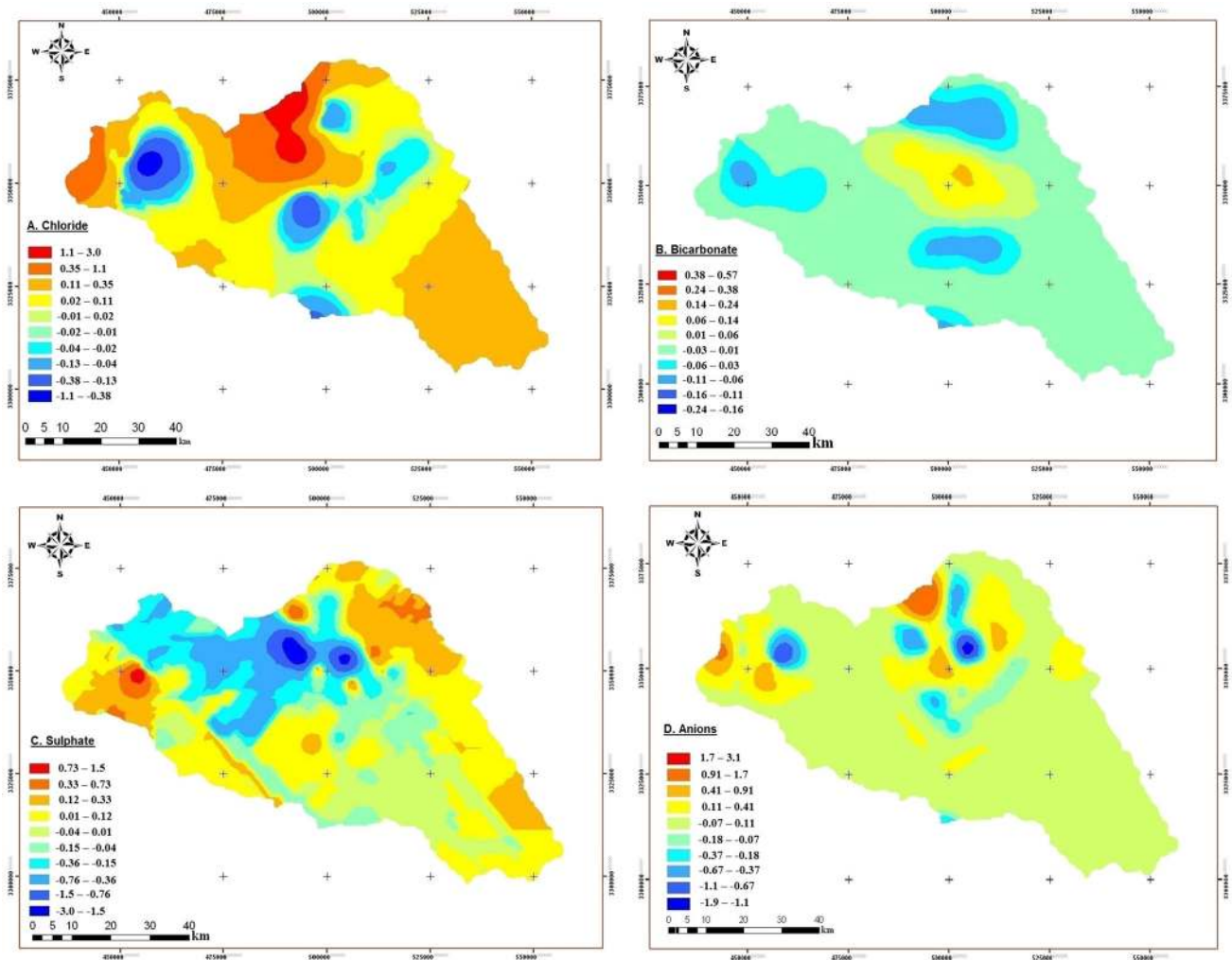


Fig. 4 Spatiotemporal mapping of RC parameter for soluble anions in Kerman aquifer including chloride (a), bicarbonate (b), sulfate (c) and total anions (d)

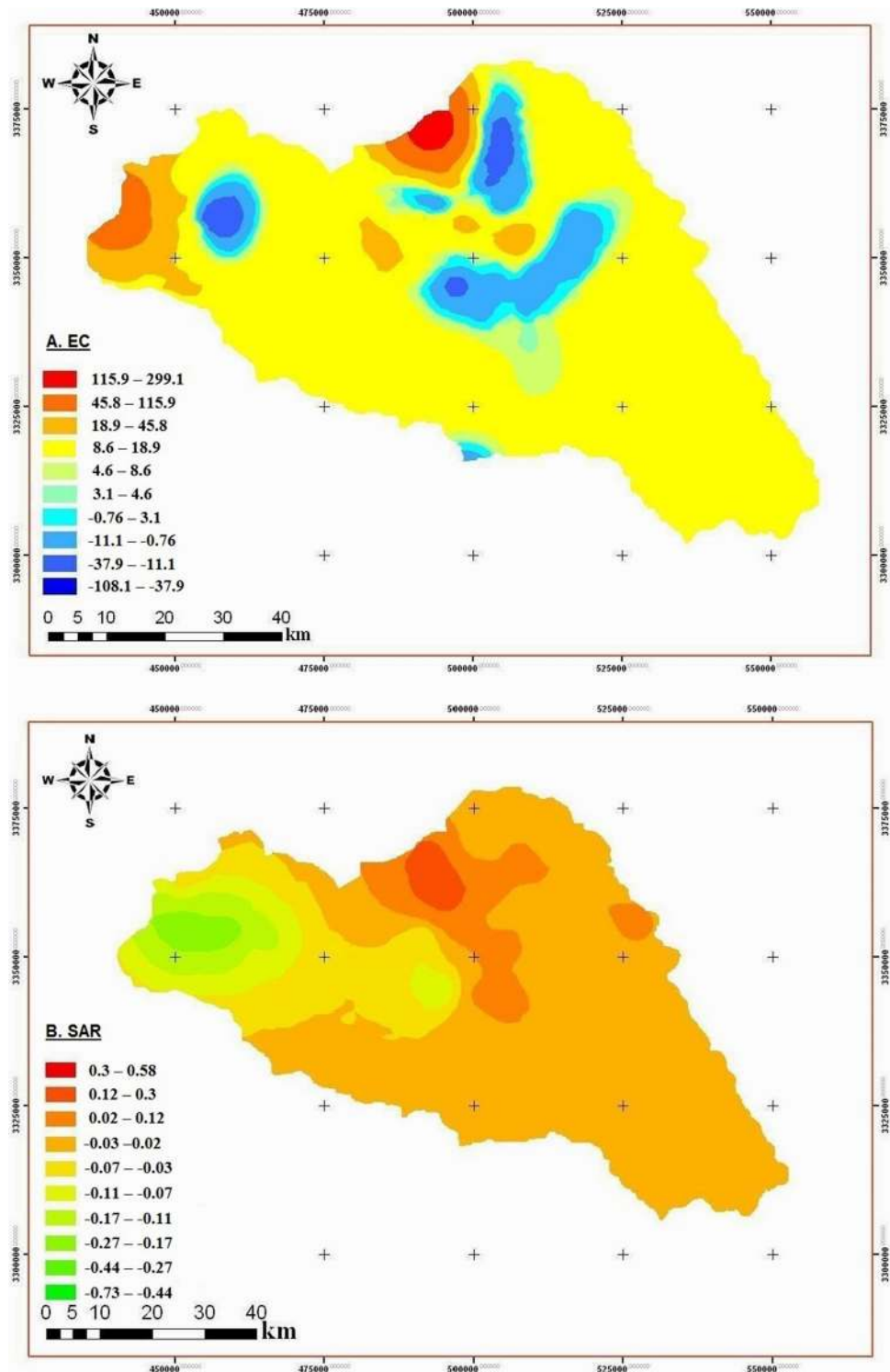
Based on correlation coefficients obtained among the RC parameters, the similarities between the sources of ions can be distinguished. Table 7 presents a simple correlation among the RC values for the groundwater irrigation qualities. The RC parameter for groundwater EC had the highest correlation coefficients with Cl^- ($r = 0.72^{**}$) and Na^+ ($r = 0.70^{**}$), afterward with Ca^{+2} ($r = 0.52^{**}$), Mg^{+2} ($r = 0.47^{**}$) and SO_4^{-2} ($r = 0.38^{**}$). Reversely, it showed no significant relationship with HCO_3^- . This can be explained partly by weathering of evaporate minerals (halite and gypsum) in the Kerman Plain (Rezaei 2013). In addition, the groundwater RC parameter for SAR showed significant relationships with Na^+ ($r = 0.74^{**}$) and Cl^- ($r = 0.33^{**}$), whereas no significant correlation was found with the other soluble ions. This finding indicated that the spatiotemporal changes of groundwater salinity (EC) and sodicity (SAR) of Kerman plain during 1999–2010 have been mainly controlled by soluble Na^+ and Cl^- .

Meanwhile, there was a positive relationship between the RC parameters of soluble Na^+ and Cl^- ($r = 0.50^{**}$).

Conclusion

Spatiotemporal mapping of Kerman groundwater variables during 1999–2010 was performed using Kriging technique combined with a linear regression approach. The result showed that among the main soluble ions, Na^+ and Cl^- had the highest concentrations in the groundwater. Except Ca^{+2} , the average concentration of all the other soluble ions and also EC were higher than the maximum permissible levels for drinking, however, Na^+ , SO_4^{-2} and EC showed no limitation for agricultural water usage. Based on the proposed RC parameter, soluble Na^+ , Ca^{+2} , Cl^- , total cations, total anions and EC have gradually increased during 1999–2010. Among the main soluble ions, Cl^- with

Fig. 5 Spatiotemporal mapping of RC parameter for EC (a) and SAR (b) in Kerman plain aquifer



0.18 meq l⁻¹ year⁻¹ showed on average the highest value of RC. Also, the groundwater EC showed an increasing trend with an average value of 16.8 $\mu\text{S cm}^{-1}$ year⁻¹. In contrast, Mg⁺², SO₄⁻² and SAR exhibited negative values of RC. The value of RC for HCO₃⁻ was zero, indicating no changes through the studied years. The geostatistics result

showed that the best method for interpolation of Na⁺, Mg⁺², Cl⁻, HCO₃⁻ and SAR was disjunctive Kriging, whereas for Ca⁺², total cations, total anions and EC, simple Kriging found to be the best method. In addition, the performance of ordinary Kriging resulted in a better interpolation for SO₄⁻². The analysis of semi-variogram indicated

Table 7 Simple correlation among regression coefficients (RC) for the groundwater properties of Kerman plain aquifer

Variable	Na ⁺	Ca ⁺²	Mg ⁺²	Cations	Cl ⁻	HCO ₃ ⁻	SO ₄ ⁻²	Anions	EC	SAR
Na ⁺	1									
Ca ⁺²	0.098 ns	1								
Mg ⁺²	0.22 ns	-0.11 ns	1							
Cations	0.80**	0.51**	0.40**	1						
Cl ⁻	0.50**	0.57**	0.04 ns	0.66**	1					
HCO ₃ ⁻	-0.16 ns	0.03 ns	-0.40**	-0.22 ns	0.07 ns	1				
SO ₄ ⁻²	0.43**	-0.005 ns	0.61**	0.48**	-0.27*	-0.57**	1			
Anions	0.80**	0.49**	0.51**	0.95**	0.63**	-0.27*	0.56**	1		
EC	0.70**	0.52**	0.47**	0.89**	0.72**	-0.18 ns	0.38**	0.92**	1	
SAR	0.74**	-0.096 ns	-0.22 ns	0.36**	0.33*	0.098 ns	0.055 ns	0.35**	0.27*	1

ns not significant

* p < 0.05

** p < 0.01

that Exponential model for Na⁺, Cl⁻, SO₄⁻², total cations and SAR, the Gaussian model for Ca⁺² and Mg⁺², and the Spherical model for HCO₃⁻, total anions and EC were the most satisfactory predictors. Nugget-to-sill ratios in the present study indicated the groundwater properties to have moderate to strong spatial structure. The minimum and maximum ranges were found for Na⁺ and SAR with the values of 7970 and 65,703 m, respectively. Comparison of the main soluble ions showed that during 1999 to 2010, the concentration of HCO₃⁻ has been increased beneath the Kerman city, whereas the reverse manner was found for Ca⁺² and SO₄⁻². The RC parameter for groundwater EC and SAR had the highest correlation coefficients with Na⁺ and Cl⁻. This finding indicated that the spatiotemporal changes of groundwater salinity (EC) and sodicity (SAR) of Kerman plain during 1999–2010 have been mainly controlled by soluble Na⁺ and Cl⁻.

References

- Aminizadeh M, Lashkaripour Gh, Ghaoori M, Hafezi N (2012) Investigation of bed rock condition of Kerman plain based on sedimentary basin model. *Irrig Water Eng* 2(7):70–82 (in Persian)
- Arslan H (2012) Spatial and temporal mapping of groundwater salinity using ordinary Kriging and indicator Kriging: The case of Bafra Plain, Turkey. *Agri Water Manage* 113:57–63
- Asadi R, Kuhi N, Yazdanpanah N (2012) Applicability of micro irrigation system on cotton yield and water use efficiency. *J food Agri Envir* 10(1):302–306
- Baalousha H (2010) Assessment of a groundwater quality monitoring network using vulnerability mapping and geostatistics: a case study from Heretaunga Plains, New Zealand. *Agri Water Manage* 97:240–246
- Dash JP, Sarangi A, Singh DK (2010) Spatial variability of groundwater depth and quality parameters in the National Capital Territory of Delhi. *Envir Manage* 45:640–650
- Delgado C, Pacheco J, Cabrea A, Baltlori E, Orellana R, Baustista F (2010) Quality of groundwater for irrigation in tropical karst environment; the case of Yucatan, Mexico. *Agri Water Manage* 97:1423–1433
- Demir Y, Ersahin S, Guler M, Cemek B, Gunal H, Arslan H (2009) Spatial variability of depth and salinity of groundwater under irrigated ustifluents in the Middle Black Sea Region of Turkey. *Envir Monitor Assess* 158:279–294
- Environmental Protection Organization of Iran (2001) Executive Law, C: No. 104, 134. The Third Development Program. Green Circe Press (in Persian)
- ESRI (2008) Using ArcGIS geostatistical analyst. Environmental Systems Research Institute, Redlands (300 pp)
- Gaus I, Kinniburgh DG, Talbot JC, Webster R (2003) Geostatistical analysis of arsenic concentration in groundwater in Bangladesh using disjunctive Kriging. *Envir Geol* 44:939–948
- Ghosh AK, Sarkar D, Dutta D, Bhattacharyya P (2004) Spatial variability and concentration of arsenic in the groundwater of a region in Nadia district, West Bengal, India. *Archives Agron Soil Sci* 50(4–5):521–527. doi:10.1080/0365034042000220757
- Guo O, Wang Y, Gao X, Ma T (2007) A new model (DRARCH) for assessing groundwater vulnerability to arsenic contamination at basin scale: a case study in Taiyuanbasin, northern China. *Envir Geol* 52(5):923–932
- Hasanpour N, Abbasnezhad A, Dadollahi H, Ghasemi Pourafshar Y (2011) Effect of water level rising on the aquifer quality of Kerman city. In: The 5th National Conference and Exhibition on Environmental Engineering. Tehran, Iran (in Persian)
- Hassanzadeh R, Abbasnejad A, Hamzeh MA (2011) Assessment of groundwater pollution in Kerman urban areas. *J Envir Stud* 36(56):31–33
- Holtz GK (2009) Seasonal variation in groundwater levels and quality under intensively drained and grazed pastures in the Montagu catchment, NW Tasmania. *Agri Water Manage* 96:255–266
- Isaaks EH, Srivastava RM (1989) An introduction to applied geostatistics. Oxford University Press, New York
- Kotuby J, Koenig R, Kitchen B (1997) Salinity and plant tolerance. Utah State University Extension, AG-SO-03, Utah
- Kravchenko AN (2003) Influence of spatial structure on accuracy of interpolation methods. *Soil Sci Soc Am J* 67:1564–1571
- Kuisi MA, Al-Qinna M, Margani A, Aljazzar T (2009) Spatial assessment of salinity and nitrate pollution in Amman-Zarqa Basin: a case study. *J Envir Earth Sci* 59:117–129

- Kumar V (2007) Optimal contour mapping of groundwater levels using universal Kriging, a case study. *Hydro Sci J* 52(5):1039–1049
- Li J, Heap AD (2008) A review of spatial interpolation methods for environmental scientists. Geoscience publication, Australia
- Maghami Y, Ghazavi R, Vali AA, Sharafi S (2011) Evaluation of spatial interpolation methods for water quality zoning using GIS Case study, Abadeh Township. *Geog Envir Plann J* 42(2):171–182 (in Persian)
- Mendes MP, Ribeiro L (2010) Nitrate probability mapping in the northern aquifer alluvial system of the river Tagus (Portugal) using Disjunctive Kriging. *Sci Total Envir* 408:1021–1034
- Moosavi AA, Sepaskhah AR (2012) Spatial variability of physico-chemical properties and hydraulic characteristics of a gravelly calcareous soil. *Archives Agron Soil Sci* 58(6):631–656. doi:10.1080/03650340.2010.533659
- Mousavifard SM, Momtaz H, Sepehr E, Davatgar N, Rasouli Sadaghiani MH (2013) Determining and mapping some soil physico-chemical properties using geostatistical and GIS techniques in the Naqadeh region, Iran. *Archives Agron Soil Sci* 59(11):1573–1589. doi:10.1080/03650340.2012.740556
- Nas B, Berktaay A (2010) Groundwater quality mapping in urban groundwater using GIS. *Envir Monitor Assess* 160(1–4):215–227
- Nazarizadeh F, Ershadian N, Zandevakili K (2006) Spatial variation of groundwater quality of Balaroud plain, Khuzestan Province. In: First Regional Conference on Optimum Utilization of Water Resources in the Karun and Zayanderud River Basins, Shahrekord University, pp 1236–1240 (in Persian)
- Neshat A, Pradhan B, Dadras M (2014) Groundwater vulnerability assessment using an improved DRASTIC method in GIS. *Reso Cons Recycl* 86:74–86
- Nourzadeh M, Mahdian MH, Malakouti MJ, Khavazi K (2012) Investigation and prediction spatial variability in chemical properties of agricultural soil using geostatistics. *Archives Agron Soil Sci* 58(5):461–475. doi:10.1080/03650340.2010.532124
- Papadopoulou-Vrynioti K, Alexakis D, Bathrellos GD, Skilodimou HD, Vryniotis D, Vassiliades E, Gamvroula D (2013) Distribution of trace elements in stream sediments of Arta plain (western Hellas): the influence of geomorphological parameters. *J Geoch Expl* 134:17–26. doi:10.1016/j.gexplo.2013.07.007
- Papadopoulou-Vrynioti K, Alexakis D, Bathrellos GD, Skilodimou HD, Vryniotis D, Vassiliades E (2014) Environmental research and evaluation of agricultural soil of the Arta plain, western Hellas. *J Geoch Expl* 136:84–92. doi:10.1016/j.gexplo.2013.10.007
- Park SJ, Vlek PLG (2002) Environmental correlation of three dimensional soil spatial variability, a comparison of three adaptive techniques. *Geoderma* 10:117–140
- Pazand K, Javanshir AR (2014) Geochemistry and water quality assessment of groundwater around Mohammadabad area, Bam district, SE Iran. *Water Qual Expo Health* 6:225–231. doi:10.1007/s12403-014-0131-9
- Rezaei M (2013) The chemical evolution of groundwater in the Kerman plain aquifer, Iran. *Int J Water* 7(1):29–43
- Rossi J, Govaerts A, Vos BD, Verbist B, Vervoort A, Poesen J, Muys B, Deckers J (2009) Spatial structures of soil organic carbon in tropical forests, a case study of Southeastern Tanzania. *Catena* 77:19–27
- Sun Y, Kang S, Li F (2009) Comparison of interpolation methods for depth to groundwater and its temporal and spatial variations in the Minqin oasis of northwest China. *Envir Model Soft* 24:1163–1170
- The Planning and Management Organization of Kerman Province (2011) Statistical yearbook of Kerman province, Iran. No. 581 (in Persian)
- Theodossiou N, Latinopoulos P (2007) Evaluation and optimisation of groundwater observation networks using the Kriging methodology. *Envir Model Soft* 21(7):991–1000
- United States Environmental Protection Agency (2012) Edition of the drinking water standards and health advisories, Washington, DC. USA, pp 12
- Wang Y, Zhang X, Huang C (2009) Spatial variability of soil total nitrogen and soil total phosphorus under different land uses in a small watershed on the Loess Plateau, China. *Geoderma* 150:141–149
- Webster R (1997) Regression and functional relations. *Eur J Soil Sci* 48:557–566. doi:10.1111/j.1365-2389.1997.tb00222.x
- Webster R, Oliver MA (2001) Geostatistics for environmental scientists. Wiley, New York
- Yang FG, Cao SY, Liu XN, Yang KJ (2008) Design of groundwater level monitoring network with ordinary Kriging. *J Hydrody* 20(3):339–346
- Yazdanpanah N, Mahmoodabadi M (2013) Reclamation of calcareous saline-sodic soil using different amendments: time changes of soluble cations in leachate. *Arab J Geosci* 6:2519–2528. doi:10.1007/s12517-011-0505-2
- Yazdanpanah N, Pazira E, Neshat A, Naghavi H, Moezi AA, Mahmoodabadi M (2011) Effect of some amendments on leachate properties of a calcareous saline-sodic soil. *Int Agroph* 25(3):307–310
- Yazdanpanah N, Pazira E, Neshat A, Mahmoodabadi M, Rodríguez Sinobas L (2013) Reclamation of calcareous saline sodic soil with different amendments (II): impact on nitrogen, phosphorous and potassium redistribution and on microbial respiration. *Agri Water Manage* 120:39–45. doi:10.1016/j.agwat.2012.08.017
- Yimit H, Eziz M, Mamat M, Tohti G (2011) Variations in groundwater levels and salinity in the Ili River Irrigation Area, Xinjiang, Northwest China: a geostatistical approach. *Int J Sustain Dev World Ecol* 18(1):55–64
- Zehtabian Gh, Janfaza E, Mohammad Asgari H, Nematollahi MJ (2010) Modeling of ground water spatial distribution for some chemical properties (case study in Garmsar watershed). *Iranian J Range Desert Res* 17(1):61–73 (in Persian)